

SUPPLEMENTARY MATERIAL FOR:

Characterization of DNA binding by the isolated N-terminal domain of vaccinia virus DNA topoisomerase IB

Benjamin Reed^{1,2}, Lyudmila Yakovleva³, Stewart Shuman³ and Ranajeet Ghose^{1,2,4,5*}

¹Department of Chemistry and Biochemistry, The City College of New York, New York, NY 10031.

Graduate Programs in ²Chemistry, ⁴Biochemistry and ⁵Physics, The Graduate Center of CUNY, New York, NY 10016.

³Molecular Biology Program, Sloan-Kettering Institute, New York, New York 10021, USA.

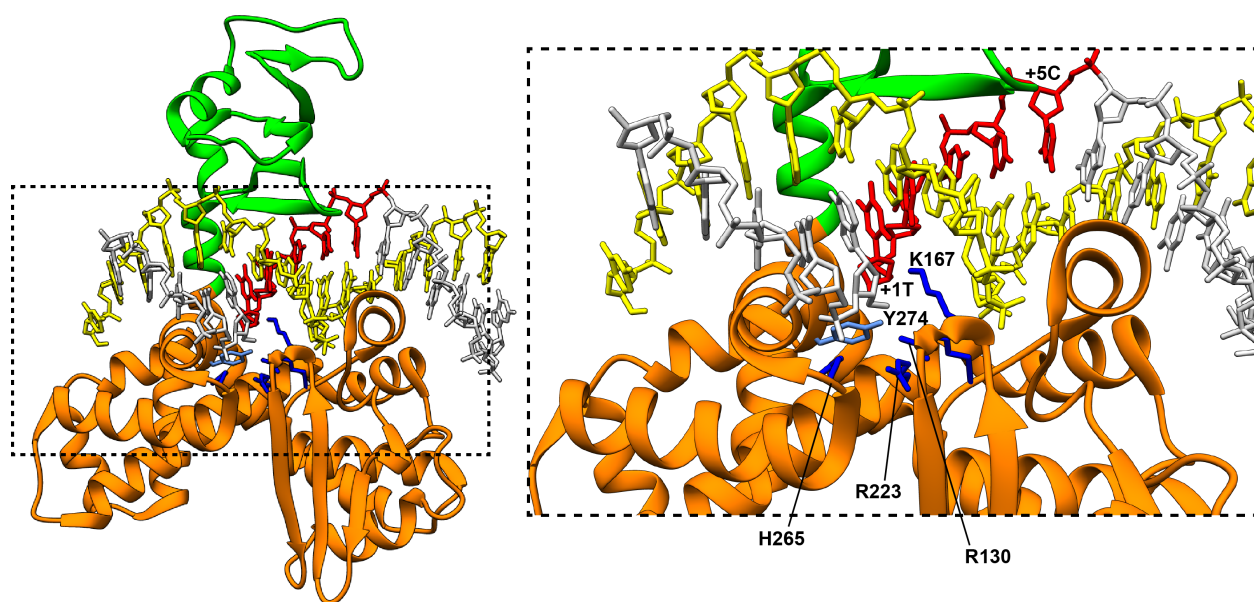


Figure S1. Interaction of full-length vTopIB (from variola virus; differs from vaccinia virus vTopIB by 3 amino acids) with DNA in the complex with an intact DNA duplex with the scissile phosphate replaced by a vanadate moiety (transition-state mimic, PDB: 3IGC). The N and C domains have been colored green and orange, respectively. The non-scissile and scissile strands of the DNA duplex have been colored yellow and light grey, respectively. The specificity element on the scissile strand (CCCTT) has been colored red. The right panel shows an expansion of the boxed region from the left panel. The 5'-terminal C (+5C) and the 3'-terminal T (+1T) of the specificity element are labeled. The sidechains of the active site residues (R130, K167, R223, H265) are shown in blue and labeled. Also shown in light blue (and labeled) is the sidechain of the tyrosine nucleophile (Y274).

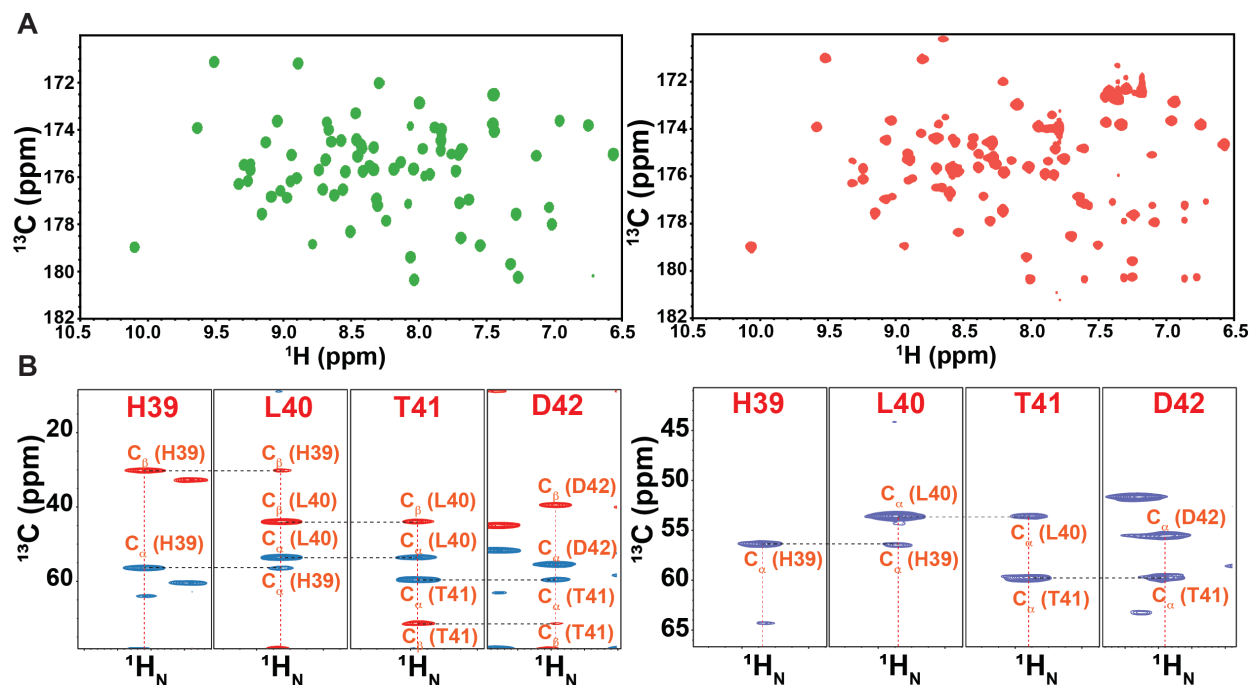


Figure S2. (A) ^{13}C , ^1H 2D projections of 3D HNCO spectra of apo TopN (600 MHz; left) and TopN in the presence of spDNA (TopN:spDNA ratio 1:2, 700 MHz; right). (B) Backbone walks for the H39-D42 segment in a CBCANH spectrum of apo TopN (600 MHz, left) and a HNCA spectrum of its spDNA complex (TopN:spDNA ratio 1:2, 700 MHz; right).

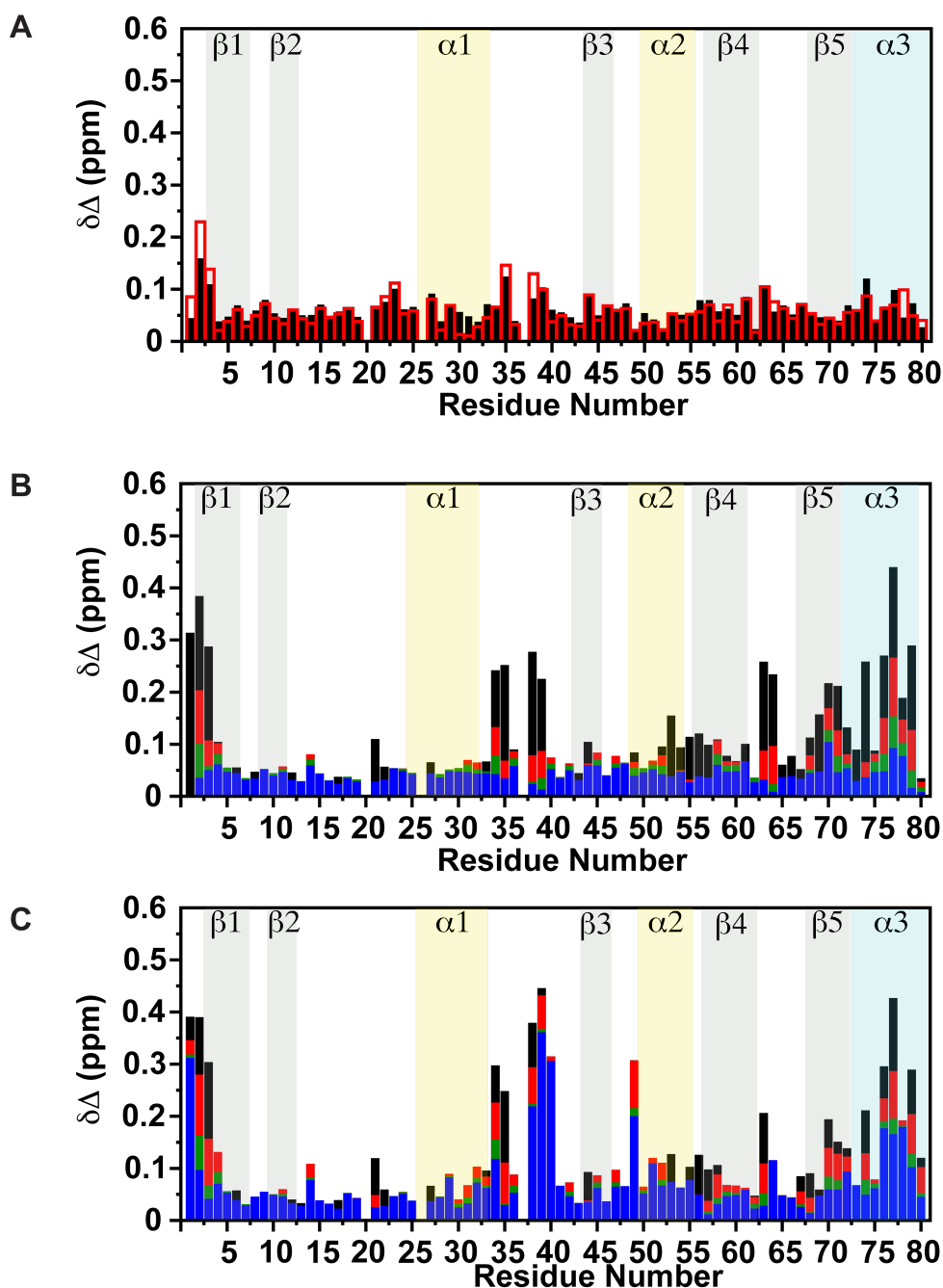


Figure S3. (A) Chemical shift perturbations induced in apo TopN by 150 mM NaCl (black solid bars) and by 150 mM NaCl + 50 mM phosphate (red open bars). Chemical shift perturbations induced on TopN by two molar equivalents of spDNA (B) or nsDNA (C) in NMR buffer containing 0 (black), 50 mM (red), 100 mM (green), or 150 mM (blue) NaCl. The chemical shifts are referenced to TopN alone in NMR buffer containing a corresponding amount of salt.

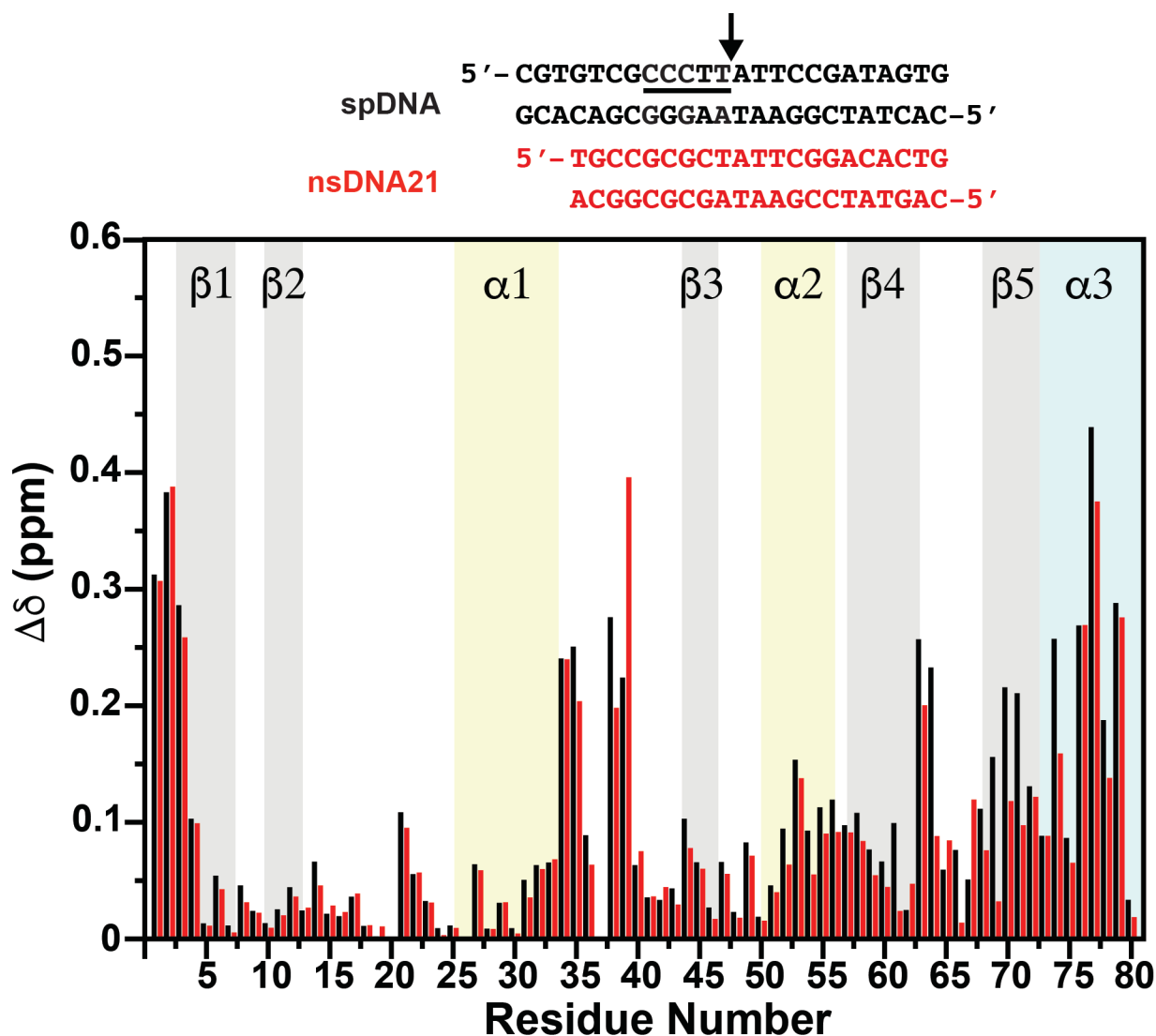


Figure S4. Comparison of chemical shift perturbations (red) induced on TopN by a 21-mer DNA duplex (nsDNA21) with little similarity to spDNA (or nsDNA) compared to shifts induced by spDNA (black). The TopN:DNA ratio was 1:2 in both cases. As in the case of nsDNA, the largest differences in the perturbations can be found in the α 1- β 3 loop. A comparison of the spDNA and the 21-mer nsDNA sequences is shown at the top. The arrow indicates the cleavage site on spDNA. Also compare Figure 4.

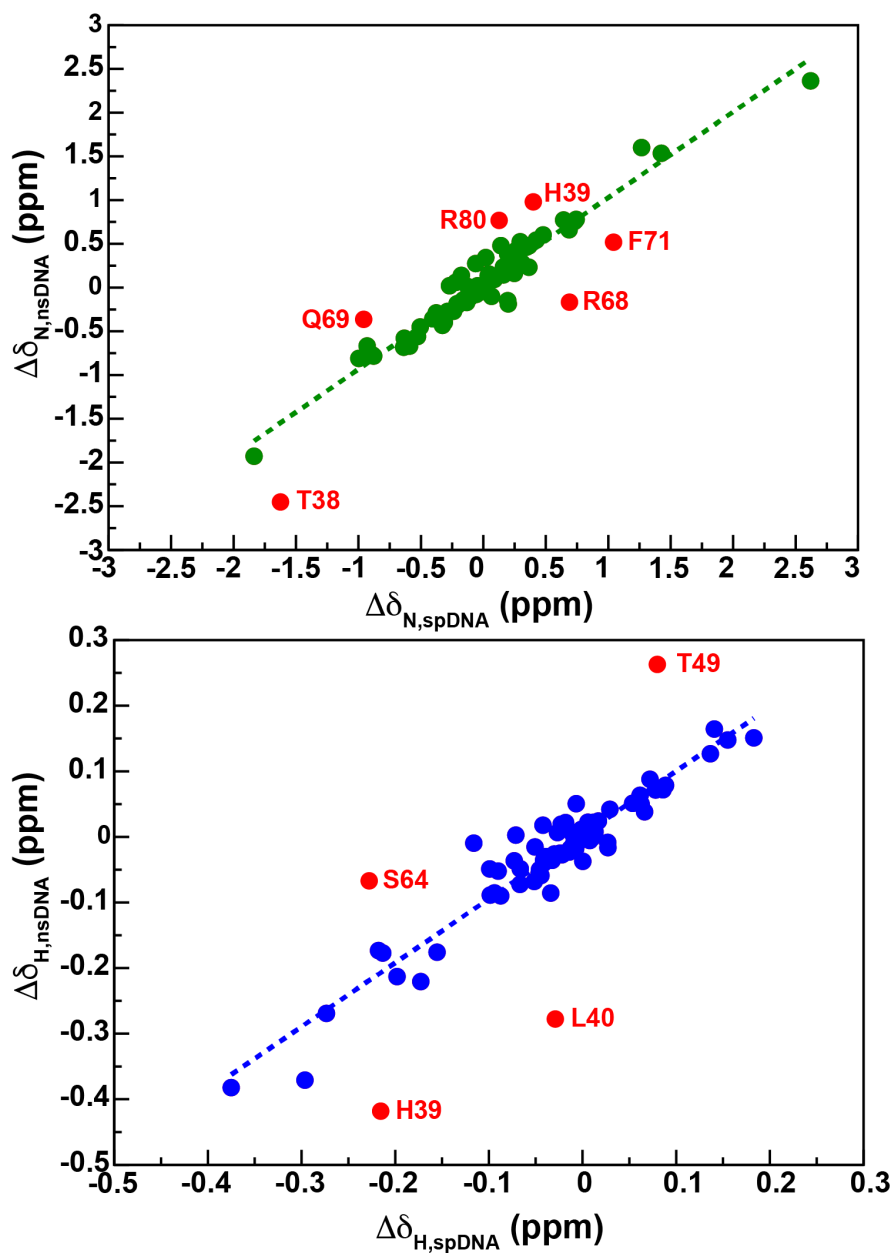


Figure S5. Correlation between amide ^{15}N (top) and ^1H (bottom) chemical shifts of TopN in the presence of spDNA or nsDNA (TopN:DNA ratio 1:2) using the corresponding apo TopN resonance position as reference. The outliers (labeled) shown as red circles were excluded from the linear regression analysis.

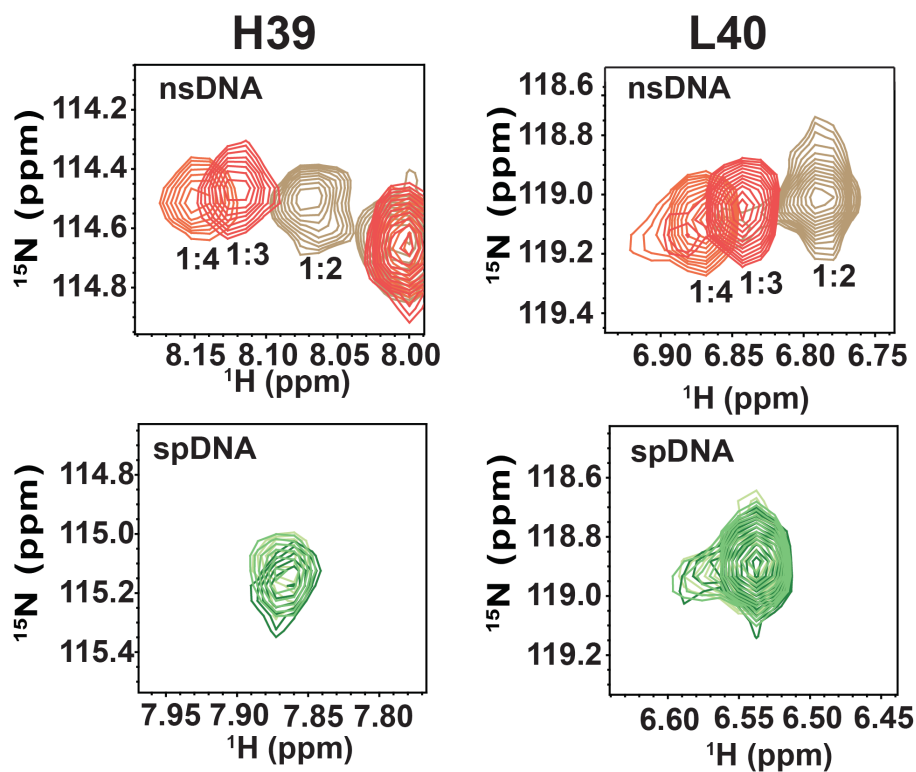


Figure S6. Expanded view of the H39 and L40 resonances in ^{15}N , ^1H HSQC spectra (800 MHz) of TopN in the presence of 2, 3 and 4 molar equivalents of nsDNA (top) or spDNA (bottom). The spectra in the presence of spDNA indicate saturation at around 2 molar equivalents, while the spectra in the presence of nsDNA suggest additional changes beyond 2 molar equivalents.

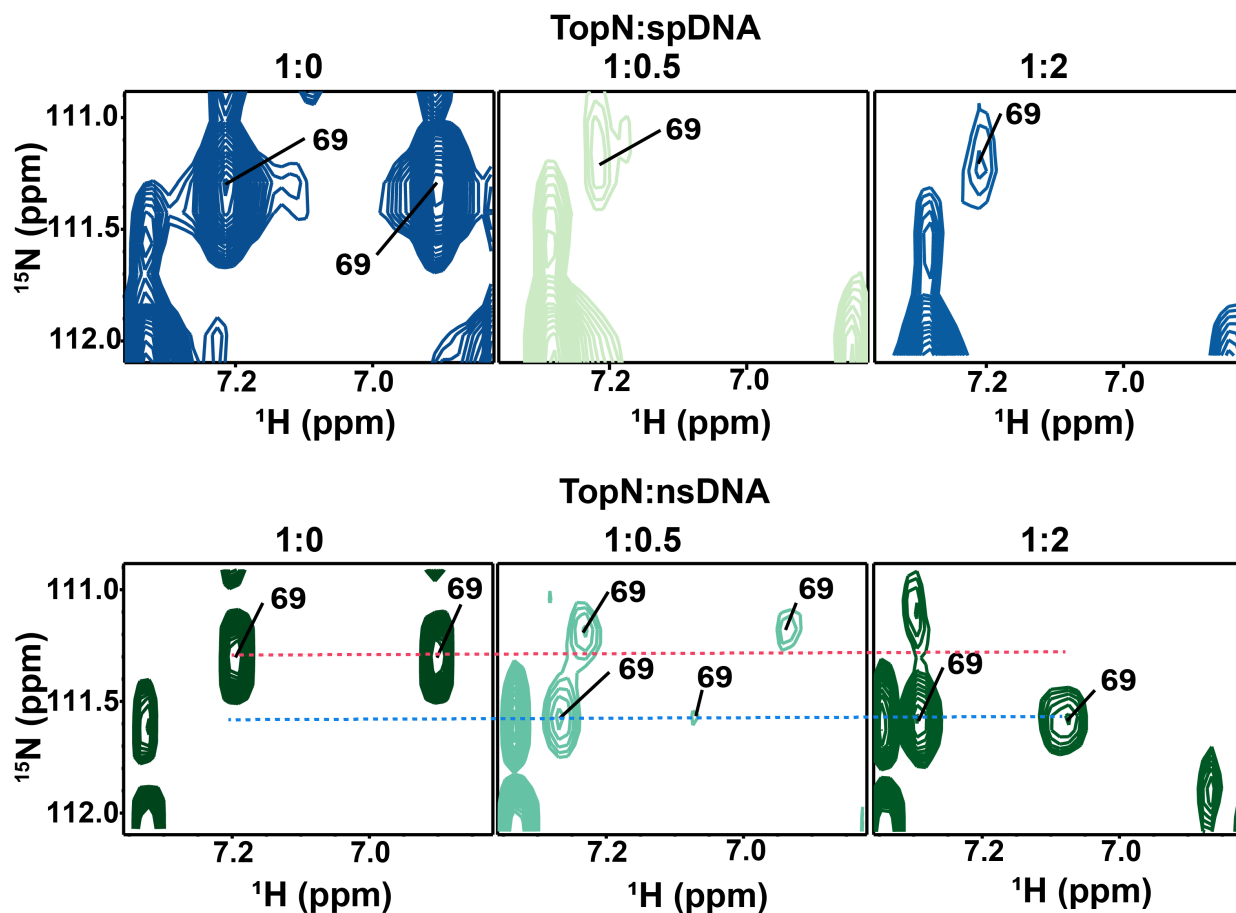


Figure S7. Comparison of the behavior of the Q69 sidechain amino (ϵ) resonances in the presence of duplex DNA. In a ^1H , ^{15}N HSQC spectrum (600 MHz) at a 1:0.5 protein:spDNA ratio, the upfield resonance for the Q69 ϵ position is completely broadened out and the downfield resonance, while broadened significantly, is still visible. No further change in the resonances is seen for a TopN:spDNA ratio of 1:2. In contrast, for a TopN:nsDNA ratio of 1:0.5 (800 MHz), two sets of resonances (signifying slow exchange on the chemical shift timescale) are seen corresponding to the Q69 ϵ position, with one set lying close to the original pair of resonances. At a TopN:nsDNA ratio of 1:2, the new set of resonances intensify and only the downfield resonance for the set close to the apo state is visible, as in the case with spDNA. The red and blue dashed lines represent the ^{15}N positions for the old and new resonances.

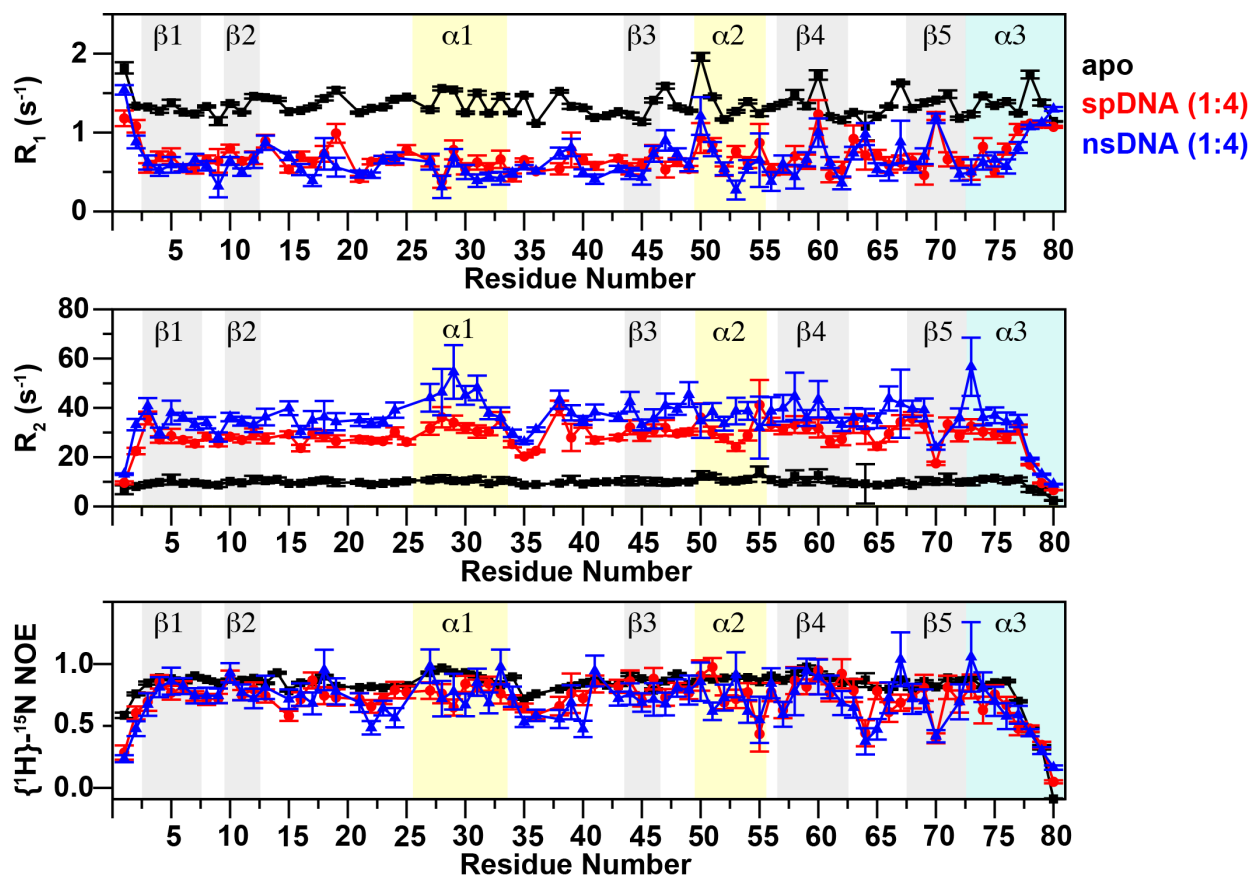


Figure S8. Backbone ^{15}N relaxation rates (R_1 , R_2 and steady-state $\{^1\text{H}\}-^{15}\text{N}$ NOE) for apo TopN and those in the presence of either spDNA (red) or nsDNA (blue) in a (TopN:DNA ratio = 1:4). Data were acquired at 800 MHz at 25 °C.

Table S1. TopN contacts with dsDNA seen in the various crystal structures of vTopIB

Residue	DNA position	PDB Structure			DNA Side Interactions		
		3IGC Bond Distance (Å)	2H7G Bond Distance (Å)	2H7F Bond Distance (Å)	Phosphate Backbone	Sugar	Base
K35	Between -2/-3	3.0	n/a	n/a	H	-	-
H39	-1(sugar), Between -1/-2	3.3	4.4	3.8	H	V	-
K65	Between +1/+2	3.1	4.7	3.5	H	-	-
R67	Between +1/+2	2.6, 3.1	2.5, 3.0	2.9, 3.2	H	-	-
Q69	+2	2.8, 3.1	2.9, 3.1	3.0, 3.5			H, H
Y70	Between +4/+5, +2:+3 (base), +3 (sugar)	2.7	2.6	2.8	H	V	V, V
Y72	Between +3/+4, +2:+3 (base), +3 (sugar)	2.8	2.7	2.8	H	V	V, V
H76	Between +2/+3	2.7	2.8	2.8	H	-	-
R80	+1 (base), Between +2/+3	3.0, 3.1	2.8, 2.9	3.0, 3.2	H, H	-	V

Residues above the dashed line make contact with the non-scissile strand of DNA; those below make contact with the scissile strand. Distances have been calculated using the sidechain N and the DNA backbone O except in the case of Q69. For the Q69 sidechain, Nε2/N7 and Oε1/N6 distances with the +2A base are shown. No backbone amide contacts are seen in the interaction of TopN and dsDNA. Distances involving K35 in the structures corresponding to PDB IDs 2H7G and 2H7F are not available since the DNA is not present at a location to enable contact.

H: hydrogen bond, V: van der Waals contact